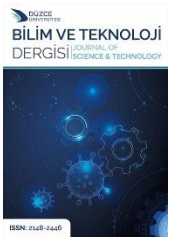

**Düzce University**
**Journal of Science & Technology**

https://dergipark.org.tr/tr/pub/dubited

*Research paper*

# *Hybrid Color Space and GLCM Feature Extraction Based Classification Method for Underwater Image Analysis*

*Nafiye Nur Apaydin*[a], *Gülşah Karaduman*[b,*], *Orhan Yaman*[a]

[a]Firat University, Faculty of Technology, Department of Digital Forensic Engineering, Elazig, Türkiye.
[b]Firat University, Faculty of Engineering, Department of Computer Engineering, Elazig, Türkiye.
[*]**Corresponding author:** gkaraduman@firat.edu.tr

**Article information:**
Received: 04/03/2025, Revision: 02/09/2025, Accepted: 05/09/2025
DOI: 10.29130/dubited.1651026

## ABSTRACT

In cases where man-made fishing nets are forgotten or lost underwater, these nets are called ghost nets. These ghost nets threaten the underwater ecosystem over time and reduce the biodiversity of living creatures underwater. For this reason, studies are being carried out to detect ghost nets underwater. In this study, SODD and Trash Icra data sets were used to detect net, trash, ROV and biological creature classes underwater. For each class, features were extracted using the GLCM filter and HSV, YUV, LAB and RGB color spaces. The extracted features were trained with the Random Forest Classification Algorithm and the results were obtained. As a result of the training, it was seen that although each color space had a low accuracy value on its own, when used together, it affected the performance positively and increased the accuracy, and the best accuracy value was 89.16% in the proposed method (HSV + YUV + LAB + RGB + GLCM). In addition, for the best case where all color spaces were used, Naive Bayes(NB), KNN and SVM classification algorithms were applied and the results were compared with the proposed method, Random Forest Classification. Accuracy values of 52% with NB, 62.17% with KNN and 73.67% with SVM were obtained and it was proven that the best method was the proposed method, Random Forest Classification algorithm. The results of the study demonstrate the effectiveness of integrating multi-color space features with texture analysis for underwater object classification, offering a promising approach for ghost net detection in real-world scenarios. Ghost nets, which are abandoned or lost man-made fishing nets, pose a significant threat to the marine ecosystem by entangling and endangering underwater life.

***Keywords:*** *GLCM Filter, HSV, RGB, YUV, LAB Color Spaces*

## I. INTRODUCTION

71% of the world consists of various water sources such as seas, oceans, and rivers. Water, which covers such a large area, is one of the important sources of life for all living things and the earth. The ecosystem of places with water is lively and has high biodiversity. At the same time, the underwater world is always intriguing. Although technology develops day by day, only a small part of the underwater world has been discovered today. Thanks to the discovery of the underwater, unknown species and ecosystems, wrecks and debris, and buried cities under water are being examined. Underwater exploration has economic and scientific contributions. For these reasons, underwater exploration is increasing day by day. However, one of the biggest and fundamental problems people face in underwater exploration is that underwater images are not clear. The underwater might appear hazy due to a number of factors, including the density of the soil in the water and the decrease in light as the water depth increases. Figure 1 provides examples of factors affecting underwater images.

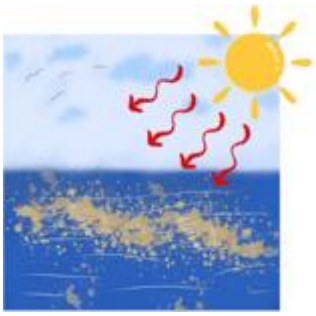

Figure 1. Factors affecting underwater images

The clarity of each underwater image varies depending on its environmental and climatic conditions. Example underwater images are given in Figure 2.

Figure 2. Sample underwater images

Underwater image processing methods are being developed to make underwater images clearer and more understandable to the human eye. The first underwater imaging study was conducted by Louis Boutan in the 1850s. The first colored underwater photographs were published in National Geographic magazine in 1927 (Apaydın et al., 2022). In the literature, there are studies on image enhancement, diver, garbage and marine waste, fish, coral, underwater plant species, object detection/classification such as wreckage images, underwater robot and submarine tracking and detection, underwater diver pose detection, spectrogram analysis, cave and view detection. Some studies in the literature on underwater are given in Table 1.

Table 1. *Some studies in the literature about underwater*

| Reference | Year | Purpose of the Study |
|---|---|---|
| (Apaydın et al., 2022) | 2022 | This paper suggests a technique for detecting underwater forensic evidence that is based on LBP (Local Binary Pattern) and SVM (Support-Vector Machine). 3552 images were collected to test the proposed method. These images consist of three classes: forensic evidence, living beings and garbage. Approximately 78.99% success was achieved with the proposed method. |
| (Demir & Yaman, 2024a) | 2024 | This work suggests a technique for detecting underwater trash that is based on KNN and HOG feature extractor. Using the publicly available Trash-ICRA19 dataset, the suggested technique achieves an accuracy of 97.78%. |
| (Han et al., 2020) | 2020 | In order to improve underwater vision, this study combines the maximum RGB and grayscale methods. A CNN (Convolutional Neutral Network) method is then suggested to address the issue of underwater images having poor illumination, and it trains the mapping relationship to produce the illumination map. Following image processing, a deep CNN approach is suggested to achieve underwater detection and classification based on underwater vision features. At 90% Map, the detecting speed is roughly 50 fps. |

Table 1 *(cont.)*. *Some studies in the literature about underwater*

| | | |
|---|---|---|
| (Demir and Yaman, 2024b) | 2024 | A projector deep feature extraction based rubbish image classification model employing underwater photos was presented in this study, which used a hybrid underwater dataset comprising 13,089 300x300 images of garbage and marine wildlife. |
| (Yuh & West, 2001) | 2001 | This study describes the current state of the art in underwater robotics, focusing on some key subsystems. |
| (De Langis et al., 2020) | 2020 | In this study, a dataset consisting of 105,000 annotated diver images was created for diver detection. Then, using this dataset, deep networks such as SSD, Faster R-CNN and YOLO were trained with Mobilenet. As a result, SSDs or Tiny-YOLOv4 were proposed for real-time applications on robots. |
| (Valdenegro-Toro, 2016) | 2016 | In order to identify underwater marine debris using Forward Looking Sonar (FLS) photos, this paper suggests using Autonomous Underwater Vehicles. |
| (Wei et al., 2024) | 2024 | This work used field-adaptive approaches to discover unattended underwater shipwrecks in side-scan sonar pictures. |
| (Character et al., 2021) | 2021 | The objective of this research is to develop a novel deep learning model implementation that automatically and quickly detects shipwrecks across a wide geographic area using digital elevation data. Shipwreck data for the United States and free source topo-bathymetric data from NOAA are utilized in conjunction with the Yolov3 architecture. The accuracy is 0.90 and the F1-Score is 0.92. |
| (Raveendran et al., 2021) | 2021 | This study examines underwater image enhancement algorithms. |

Unfortunately, the underwater world is under threat as a result of some human activities. Examples of these human activities include dumping all kinds of garbage and chemical waste into the sea, and abandoned, lost, and forgotten ghost nets developed for the purpose of catching underwater creatures such as fish (Zuzanna et al., 2022). These ghost nets remain underwater for a long time, threatening the underwater ecosystem. The biodiversity of underwater creatures such as underwater turtles and fish is decreasing due to these nets. Figure 3 shows examples of marine creatures exposed to ghost nets.

Figure 3. Marine creatures caught in ghost nets

In addition, ghost nets can be an obstacle for ships and the micro plastic waste that forms as a result of their dissolution can harm the ecosystem. Detection of ghost nets is of vital importance to maintain the order of the underwater ecosystem. However, since these nets are many times deeper in the sea, it is difficult to detect them with human power. Therefore, technology is used to detect these nets.
Unlike previous research, this study aims to identify live, trash, and ROVs in addition to identifying forgotten and submerged nets. Table 2 provides some studies in the literature that are similar to the subject of underwater net detection.

Table 2. *Some studies in the literature on underwater net detection.*

| Reference | Year | Purpose of the Study |
|---|---|---|
| (Morishige & McElwee, 2012) | 2012 | The purpose of this study was to identify and eliminate derelict fishing gear (DFG). Because of past and present DFG research in the area, it focuses on the North Pacific Ocean, especially the Hawaiian Archipelago. |
| (Zhang et al., 2024) | 2024 | 95.49% accuracy was attained in this study's suggested masked guided deep learning fishing net detection and recognition system, which is based on underwater range-gated laser imagery. |
| (Zhao et al., 2020) | 2020 | Based on non-contact underwater and image processing technologies, this study proposes an adaptive damage detection approach for fishing nets that can accurately identify damaged nets, assess the extent of underwater net damage, and restore the damaged position. |
| (Spirkovski et al., 2019) | 2019 | A pilot research was carried out in Lake Ohrid, Macedonia, to determine the prevalence of abandoned, lost, or otherwise discarded fishing equipment (ALDFG). |
| (Rijkure et al., 2024) | 2024 | The aim of this study is to review innovative robotic methods of releasing ghost networks and to present solutions that can improve this process. |
| (Ye & Wang, 2018) | 2018 | To guarantee the accuracy of fishing net detection, a novel underwater laser scanning technology is introduced in this work to gather clear and high-precision fishing net data. |
| [17] | 2022 | Basic definitions and information about illegal, unreported, and unreported fishing, as well as its effects, such as ghost fishing, are provided in this paper. |
| (Kim et al., 2019b) | 2019 | In this study, a ghost network recovery technique that can automatically identify, identify, and eliminate ghost networks is created along with a small agent tool for manipulation purposes. This tool is used to complete the ghost network recovery process. |
| (Kim et al., 2019a) | 2019 | This research proposes a mini-ROV-based underwater manipulation system for phantom net and other difficult object recovery tasks. |

## II. MATERIAL METHOD

### *A. Datasets*

In this study, two publicly available datasets from the literature, SODD and Trash Icra, were used. These datasets were combined to create a new dataset consisting of four classes: Net, Rubbish, ROV, and Biological Living Creature. As the number of images in each class was not evenly distributed, 750 images were randomly selected from each class to ensure balance. Details regarding the datasets used and the data selection procedures applied t are provided below.

*A.1. SODD Dataset*

The SODD dataset is a dataset consisting of 3168 underwater images. There are a total of 8934 objects in these 3168 images. The dataset also has YOLO labels for the objects. Table 3 shows the class names and the numbers of these classes in the dataset (Imam et al., 2023).

Table 1. Class names and numbers of the SODD dataset.

| Classes | Number of Data |
|---|---|
| propeller | 1092 |
| pipe | 2008 |
| pipe_type2 | 886 |
| red_fin | 760 |
| net | 1556 |
| qr_codes | 2632 |

*A.2. Trash Icra Dataset*

5700 images from underwater recordings were labeled for classes like trash, biological items like plants and animals, and ROVs to form the Trash Icra dataset. The SODD and Trash Icra datasets' network classes were integrated and used in this investigation (Fulton et al., 2020).

*A.3. Dataset Used in the Study, Obtained by Combining SODD and Trash Execution Datasets*

In the SODD dataset, the class ID of the network class in yolo labels is 3. Using these yolo labels, only objects with ID 3, that is, only objects with the network class, were cropped. Similarly, the objects in the images in the Trash Icra dataset were cropped using the xml tags of the images. An example cropped image of the network class is given in Figure 4.


Figure 4. Cropping an example image of the Network class

The number of objects obtained for each class as a result of cropping and saving the objects in the images is given in Table 4.

Table 4. Number of cropped objects for each class used in the study.

| Class ID | Class | Number of Clipped Objects |
|---|---|---|
| 1 | Net | 778 |
| 2 | Rubbish | 6354 |
| 3 | ROV | 2274 |
| 4 | biological living creature | 2417 |

The number of cropped objects obtained is different for each class. In order to obtain more accurate results in the study, 750 objects were randomly selected from each class. An example of obtaining random images for the network class is given in Figure 5.


Figure 5. Obtaining random images for the network class

Thanks to the random selection of images, the number of object images in each class was equalized and 750 object images were provided in each class.

*B. Proposed Method*

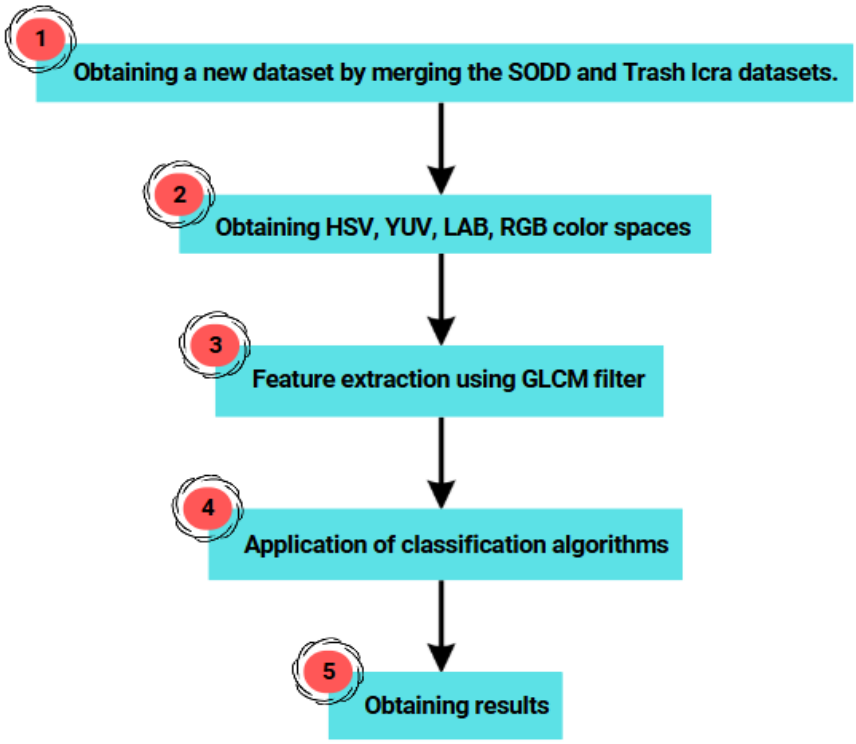


Figure 6. Flow diagram for the suggested approach

Figure 6 shows the suggested method's flow chart. According to this chart, the data set to be used was first organized. SODD and Trash Icra Data Sets were used in the study. Images belonging to the network

object were taken from the SODD data set, and images from the trash, rov and biological living classes were taken from the Trash Icra data set. The objects were cropped using the labels of these images. Since the number of cropped objects was different in each class, 750 images were randomly selected from each class in order to obtain more accurate results. In the second step, the HSV, YUV, LAB color spaces of the randomly selected images for each class were obtained. No operation was carried out to obtain the RGB color space because every image was RGB.

*B.1. HSV Color Space*

Hue, Saturation, Value, or HSV, is an intuitive representation of color and one of the color spaces that is closest to how people see color (Shaik et al., 2015; Al-Tairi, et al. 2014).

- **Layer H:** Defines the basic colors. The general representation of the basic colors is given below:
  - Red: 0° (or 360°)
  - Yellow: 60°
  - Green: 120°
  - Cyan: 180°
  - Blue: 240°
  - Magenta: 300°

- **Layer S:** It represents the purity and liveliness of color.
- **Layer V:** It represents the brightness of the color, that is, the state of being dark and light.

*B.2. Steps to Obtain HSV Color Space From RGB (Red, Green, Blue) Color Space (Shaik et al., 2015; Al-Tairi et al., 2014)*

R, G, B Layers are normalized between 0-1.

$$R' = R / 255 \quad (1)$$

$$G' = G / 255 \quad (2)$$

$$B' = B / 255 \quad (3)$$

The values obtained from the normalization process are analyzed to determine their maximum and minimum values.

$$Cmax = \max(R',G',B') \quad (4)$$

$$Cmin = \min(R',G',B') \quad (5)$$

$$\Delta = Cmax - Cmin \quad (6)$$

Layer H is calculated.

$$\text{If } \Delta = 0 \text{ than } H = 0 \quad (7)$$

$$\text{If } Cmax = R' \text{ than } H = 60 \times [((G' - B') / \Delta) \bmod 6] \quad (8)$$

$$\text{If } Cmax = G' \text{ than } H = 60 \times [((B' - R') / \Delta) + 2] \quad (9)$$

$$\text{If } Cmax = B' \text{ than } H = 60 \times [((R' - G') / \Delta) + 4] \quad (10)$$

The S layer is calculated.

$$\text{If } Cmax = 0 \text{ than } S = 0 \quad (11)$$

$$\text{Else, } S = \Delta / Cmax \quad (12)$$

The V layer is calculated.

$$V = Cmax \quad (13)$$

*B.3. YUV Color Space*

In underwater images, the ratio of blue to green is greater than the ratio of red. YUV color space can be used to eliminate red color loss (Al-Tairi et. al., 2014).

- Layer Y (Luminance): Determines the brightness of an image. Creates a black and white image.
- U and V (Chrominance): The U component of an image provides information about the blue tones, and the V component provides information about the red tones.

*B.4. Steps to Obtain YUV Color Space From RGB (Red, Green, Blue) Color Space (Al-Tairi et al., 2014)*

The R, G and B layers are normalized from 0 to 1 using Equations 1, 2, 3.
Layer Y is calculated.

$$Y = 0.299R + 0.587G + 0.114B \quad (14)$$

U Layer is calculated.

$$U = 0.492\,(B-Y) = -0.147R - 0.289G + 0.436B \quad (15)$$

V Layer is calculated.

$$V = 0.877\,(R-Y) = 0.615R - 0.515G - 0.100B \quad (16)$$

*B.5. LAB Color Space*

It is a color space created based on the human visual system, independent of the device (Yuan et al., 2021).

- Layer L (Lightness): Specifies the brightness value between Black and White (0-100).
- Layer A: It indicates the balance of red and green colors. Red color is expressed with positive values and green color is expressed with negative values.
- Layer B: It indicates the balance of yellow and blue colors. Yellow color is expressed with positive values and blue color is expressed with negative values.

*B.6. Steps to Obtain LAB Color Space From RGB (Red, Green, Blue) Color Space (Yuan et al., 2021)*

Values in the RGB color space vary depending on the color production capacity of a device. For example, RGB values on a monitor and a printer may not show the same color. Since LAB is a color space created based on the human visual system in a way that is independent of the device, when converting from RGB to LAB color space, the RGB color space must be converted to a representative color space model such as CIEXYZ that is independent of the device.

The R, G and B layers are normalized from 0 to 1 using Equations 1, 2, 3.

Gamma correction is applied to the normalized version of the R, G, B Layers.

$$\text{If } R' \le 0.04045 \text{ then } R_c = R' / 12.92 \quad (17)$$

$$\text{Else } R_c = ((R' + 0.055) / 1.055)^{2.4} \quad (18)$$

$$\text{If } G' \le 0.04045 \text{ than } G_c = G' / 12.92 \quad (19)$$

$$\text{Else } G_c = ((G' + 0.055) / 1.055)^{2.4} \quad (20)$$

$$\text{If } B' \le 0.04045 \text{ than } B_c = B' / 12.92 \quad (21)$$

$$\text{Else } B_c = ((B' + 0.055) / 1.055)^{2.4} \quad (22)$$

X, Y, Z Layers of CIE XYZ color space are calculated using R_c, G_c, B_c ‘s.

$$X = 0.4124564 * R_c + 0.3575761 * G_c + 0.1804375 * B_c \quad (23)$$

$$Y = 0.2126729 * R\_c + 0.7151522 * G\_c + 0.0721750 * B\_c \quad (24)$$

$$Z = 0.0193339 * R\_c + 0.1191920 * G\_c + 0.9503041 * B\_c \quad (25)$$

CIEXYZ values are normalized to the reference white point of the colors.

$$X\_n = 95.047, Y\_n = 100.000, Z\_n = 108.883 \quad (26)$$

$$\text{If } t > (6/29)^3 \text{ than } f(t) = t^{(1/3)} \quad (27)$$

$$\text{Else } f(t) = (1/3) * (29/6)^2 * t + 4/29 \quad (28)$$

Layer L is calculated.

$$L = 116 * f(Y / Y\_n) - 16 \quad (29)$$

Layer A is calculated.

$$a = 500 * (f(X / X\_n) - f(Y / Y\_n)) \quad (30)$$

Layer B is calculated.

$$b = 200 * (f(Y / Y\_n) - f(Z / Z\_n)) \quad (31)$$

In Figure 7, images of RGB, HSV, YUV and LAB color spaces of a sample object for each class are given.

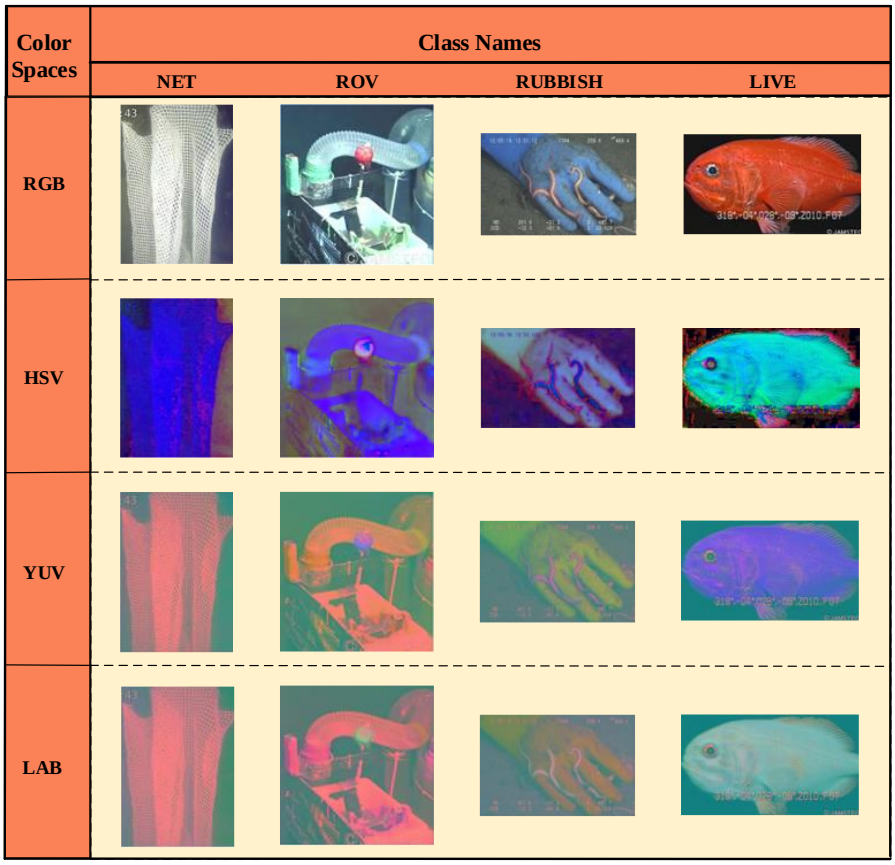


Figure 7. Image of RGB, HSV, YUV, LAB color spaces of an example object for each class

The third stage involved applying the GLCM Filter to every color space that was obtained and extracting characteristics from them.

*B.7. GLCM Filter*

The GLCM (Gray Level Co-Occurrence Matrix) filter is a method used to perform textural analysis of the gray tones of an image (Mohanaiah et al. 2013).

*B.8. Steps to obtain the features Resulting From the GLCM Filter (Mohanaiah et al. 2013)*

The picture is first turned to grayscale. The GLCM matrix is then produced.

$$P(i, j \mid d, \theta) = \text{Matrix}[((x1, y1), (x2, y2)) \in D \mid I(x1, y1) = i, I(x2, y2) = j] \quad (32)$$

I(x,y): The gray level of a pixel in an image.
D: Image coordinates.
d: Distance.
θ: Direction.

All elements of the resulting matrix are normalized.

$$P'(i,j) = P(i,j) \,/\, \sum_{i=1}^{N} \sum_{j=1}^{N} P(i,j) \quad (33)$$

In the last step, Energy, Similarity, Contrast, Homogeneity and Correlation textural features are extracted.

$$\text{Similarity} = \sum_{i=0}^{N-1} \sum_{j=0}^{N-1} P'(i,j)2 \quad (34)$$

i, j: Gray level density values.
N: The total number of gray level intensities.

$$\text{Contrast} = \sum_{i=1}^{N-1} \sum_{j=1}^{N-1} (i-j)2 \times P'(i,j) \quad (35)$$

$$\text{Homogeneity} = \sum_{i=0}^{N-1} \sum_{j=0}^{N-1} \frac{P\prime(i,j)}{1+|i-j|} \quad (36)$$

$$\text{Energy} = \sqrt{Benzerlik} \quad (37)$$

$$\text{Correlation} = \frac{\sum_{i=0}^{N-1} \sum_{j=0}^{N-1} (i-\mu i)(j-\mu j) P\prime(i,j)}{\sigma i \sigma j} \quad (38)$$

μi,μj : Averages of the gray level values in GLCM for rows (i) and columns (j).

σi,σj : Gray level value standard deviations for rows (i) and columns (j).

In the last step, the results were compared by applying the proposed method, Random Forest (RF) Classification algorithm, and NB, K-Nearest Neighbors (KNN) and Support Vector Machines (SVM) classification algorithms to the obtained GLCM features.

*B.9. RF Algorithm*

The RF is an algorithm created by combining multiple decision trees. In this algorithm, random samples are selected from the dataset to train the trees. Then, in order to be able to make branches in these trees, a set of sub-features is evaluated randomly to find the best case for division (Akbulut et al., 2025). When the best divisions and decision trees are all created, the results of all decision trees are taken and the classes are determined to fit the majority. Figure 8 shows the working logic of the RF Algorithm (Belgiu & Drăguţ, 2016).

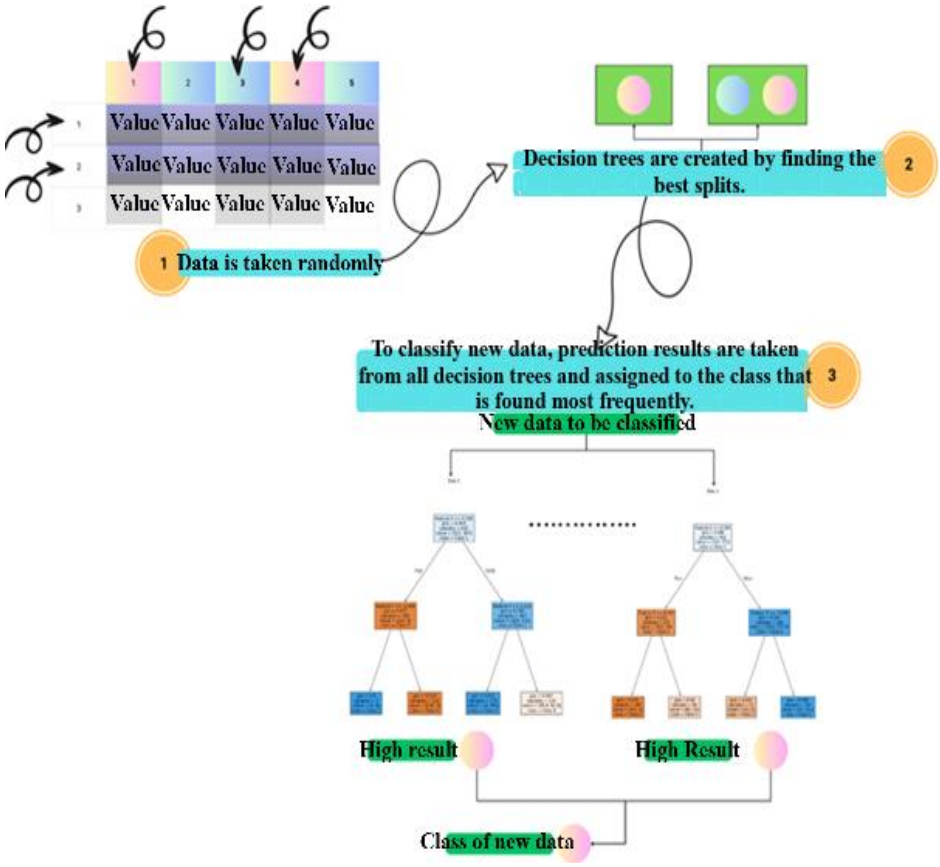


Figure 8. Working logic of RF Algorithm

*B.10. Naïve Bayes(NB) Classification Algorithm*

NB classification algorithm assumes that each feature in the data set is independent of each other. Later, when it performs classification, it evaluates the contributions of each feature to the class separately and determines which class the data belongs to as a result of the combination of these contributions (Yang, 2018).

*B.11. KNN Algorithm*

One supervised learning technique for labeled data is the KNN algorithm. In the first step; it takes random points in the data as the center and then divides the data into clusters by measuring the distance of other points to the center points with methods such as the Euclidean distance metric. In the second step, it calculates the centers of the clusters it creates and continues the clustering process by recalculating the distances of all points according to this center until no element changes. Thus, it classifies all the data (Demir & Yaman., 2024a).

*B.12. SVM Algorithm*

Finding the optimal n hyperplane that divides the classes from one another is the primary goal of SVM. As a result, the data is generalized and the distance between the classes is maximized. These distances are calculated using support vectors. Kernel functions are used to convert the data into a high-dimensional space for non-linear drawings. This improves the classification of non-linear data (Yaman et al., 2020).

Accuracy, Precision and F-1 Score parameters were used to evaluate the proposed method (Demir & Yaman, 2024b).

*B.13. Accuracy*

Accuracy is the parameter that gives the ratio of correct predictions to total predictions. It is calculated with Equation 39 (Demir & Yaman, 2024b).

$$Accuracy = (TP + TN)/(TP + TN + FP + FN) \quad (39)$$

TP: True Positives
TN: True Negatives
FP: False Positives
FN: False Negatives

*B.14. Precision*

Precision gives how accurate the predictions for the positive class actually are. It is calculated with Equation 40 (Demir & Yaman, 2024b).

$$Precision = TP/(TP + FP) \quad (40)$$

*B.15. F-1 Score*

F-1 Score provides the balance between Precision and Recall. It is the harmonic mean of Precision and Recall. It is calculated with Equation 41 (Demir & Yaman, 2024b).

$$F - 1\ Score = 2 \times (Precision\ \times Recall)/(Precision + Recall) \quad (41)$$

## III. EXPERIMENTAL RESULTS

In this study, net, trash, ROV, and living beings were detected from underwater images using HSV, YUV, LAB, RGB color spaces, GLCM filter, and RF algorithm. Then, the results of the proposed method, RF algorithm, were compared with NB, KNN, and SVM classification algorithms. 10-fold cross validation was used for validation in each method. The host computer's Pycharm code editor and Google Colab, a cloud service built on the Python programming language, were used to implement the suggested approach. With the Pycharm code editor, objects were cropped and their features were extracted by applying the GLCM filter. The features derived from the GLCM filter were used to train the NB, KNN, SVM, and RF algorithms using Google Colab. Table 5 lists the hardware features, packages, and libraries used in the investigation.

Table 5. Features of libraries, packages and hardware used in the study

| Software and Libraries | Values |
|---|---|
| Google Colab | - |
| Pycharm | 2024.3.1 |
| Python | 3.13.1 |
| Numpy | 2.2.0 |
| OpenCV | 4.10.0.84 |
| Pandas | 2.2.3 |
| Matplotlib | 3.10.0 |
| Pillow | 11.0.0 |
| scikit-learn | 1.6.0 |
| openpyxl | 3.1.5 |
| System | Intel(R) Core(TM) i5-3230M |
| CPU | 2.60GHz |

Confusion matrices obtained as a result of training the features obtained by applying the GLCM filter for each combination of color spaces with the proposed method, RF, are given in Figure 9.

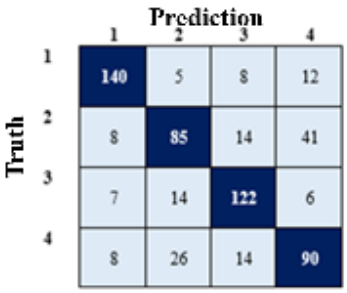


a) HSV

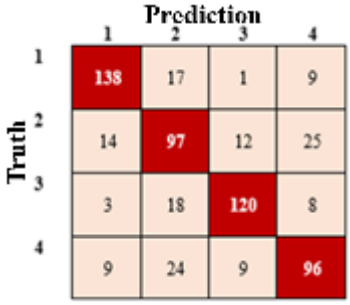


b) YUV

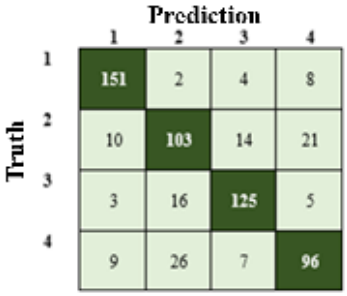


c) LAB

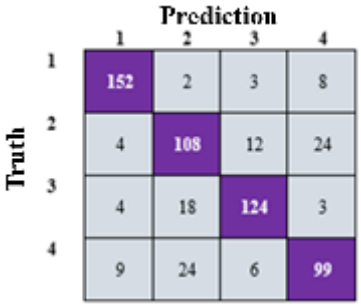


d) RGB

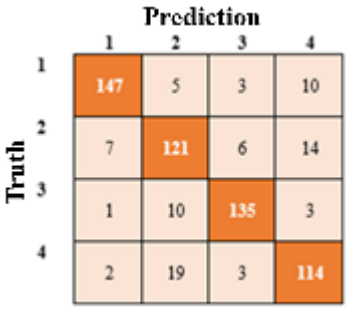


e) HSV + YUV

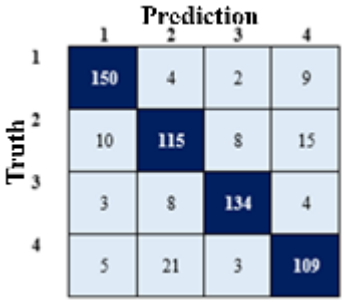


f) HSV + LAB

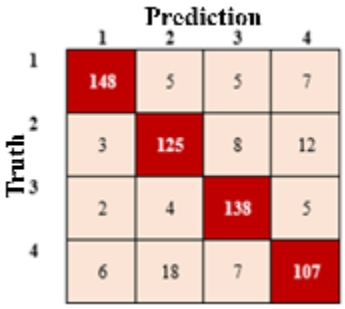


g) HSV + RGB

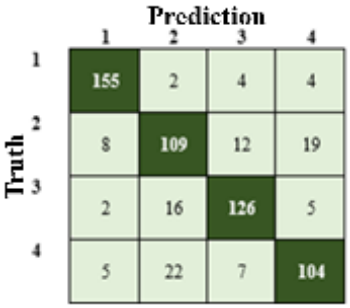


h) YUV + LAB

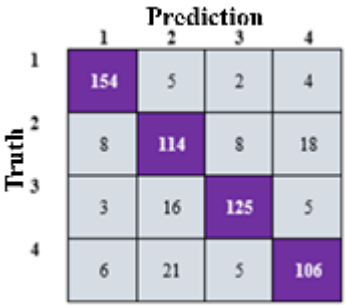


i) YUV + RGB

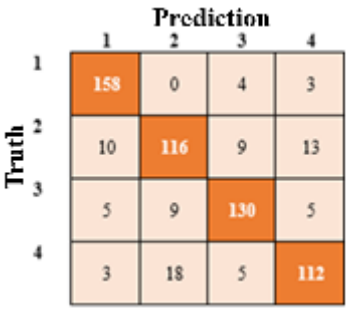


j) LAB + RGB

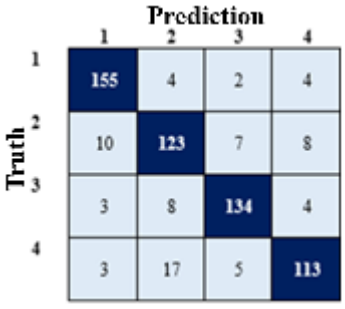


k) HSV + YUV + LAB

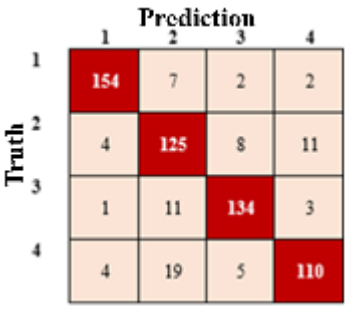


l) HSV + YUV + RGB

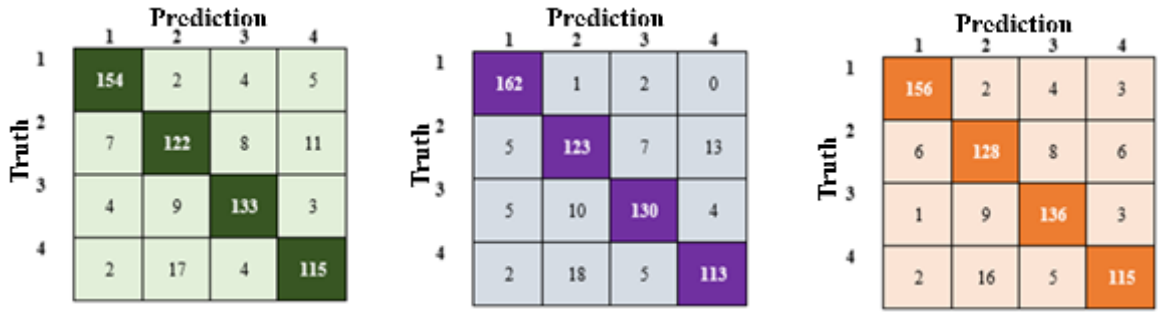


**m) HSV + LAB + RGB** **n) YUV + LAB + RGB** **o) HSV + YUV + LAB + RGB**

Figure 9. Confusion matrices of the proposed method for all combinations of color spaces: a) HSV, b) YUV, c) LAB, d) RGB, e) HSV + YUV, f) HSV + LAB, g) HSV + RGB, h) YUV + LAB, i) YUV + RGB, j) LAB + RGB, k) HSV + YUV + LAB, l) HSV + YUV + RGB, m) HSV + LAB + RGB, n) YUV + LAB + RGB, o) HSV + YUV + LAB + RGB

A confusion matrix is a tabular structure used to evaluate the performance of a model in classification problems, comparing the true and predicted classes. This matrix allows the calculation of metrics such as the accuracy, sensitivity, and specificity of the model by showing values such as true positives, false positives, true negatives, and false negatives. Figure 9 presents the confusion matrices corresponding to different color space combinations employed in the proposed method. Using a single color space alone—such as HSV (Figure 9a), YUV (Figure 9b), LAB (Figure 9c), or RGB (Figure 9d)—results in lower classification performance, particularly due to increased misclassifications among visually similar classes. Combining two color spaces enhances classification accuracy, as illustrated in Figures 9e to 9j. Among these dual combinations, HSV + LAB (Figure 9f) and YUV + LAB (Figure 9h) yield relatively more balanced results with fewer misclassifications across all classes. Notably, employing three color spaces (Figure 9k) significantly improves classification performance. The combination HSV + YUV + LAB achieves high accuracy with the most prominent diagonal values and minimal off-diagonal errors, demonstrating enhanced feature representation. Most importantly, the best classification performance is achieved when all four color spaces (HSV + YUV + RGB + LAB, Figure 9o) are combined. The confusion matrix clearly indicates that integrating all color spaces provides complementary information that maximizes the model's discriminative capability. This finding confirms that multi-space color feature integration plays a crucial role in enhancing both the robustness and accuracy of the classification process.

Following 100 iterations of the suggested procedure, Table 6 provides the Accuracy, Precision, and F1-Score performance values for each combination of color spaces.

Table 6. Accuracy, Precision and F-1 Score values of the RF method for each color space

| **Color Spaces** | **Accuracy (%)** | **Precision (%)** | **F1-Score (%)** |
|---|---|---|---|
| HSV | 72.83 | 72.82 | 72.72 |
| YUV | 75.17 | 75.46 | 75.29 |
| LAB | 79.17 | 78.97 | 79.03 |
| RGB | 80.5 | 80.49 | 80.48 |
| HSV + YUV | 86.17 | 86.41 | 86.26 |
| HSV + LAB | 84.67 | 84.66 | 84.66 |
| HSV + RGB | 86.33 | 86.36 | 86.30 |
| YUV + LAB | 82.33 | 82.24 | 82.27 |

Table 6 (cont.). Accuracy, Precision and F-1 Score values of the RF method for each color space

| | | | |
|---|---|---|---|
| YUV + RGB | 83.17 | 83.30 | 83.18 |
| LAB + RGB | 86 | 85.88 | 85.90 |
| HSV + YUV + LAB | 87.5 | 87.52 | 87.48 |
| HSV + YUV + RGB | 87.17 | 87.43 | 87.22 |
| HSV + LAB + RGB | 87.33 | 87.33 | 87.32 |
| YUV + LAB + RGB | 88 | 87.98 | 87.94 |
| **HSV + YUV + LAB + RGB** | **89.17** | **89.27** | **89.17** |

When Figure 9 and Table 6 are examined, it is seen that each color space used has low accuracy rates alone. Accordingly, the lowest accuracy rate alone is in the HSV color space. The RGB color space has the highest accuracy rate on its own. Nevertheless, it has been found that combining the four color spaces improves performance and results in greater accuracy values. The best accuracy value of these values is 89.17% in the proposed method, that is, by using combinations of all color spaces.

Since the combination where all color spaces are used together is the best; SVM, KNN and NB algorithms are also applied for this combination and compared with RF.

In Figure 10, the confusion matrix of the NB, KNN, SVM, RF classification algorithms for the combination where all color spaces are used is given, and their Accuracy, Precision, F1-Score performance metrics are given in Table 7.

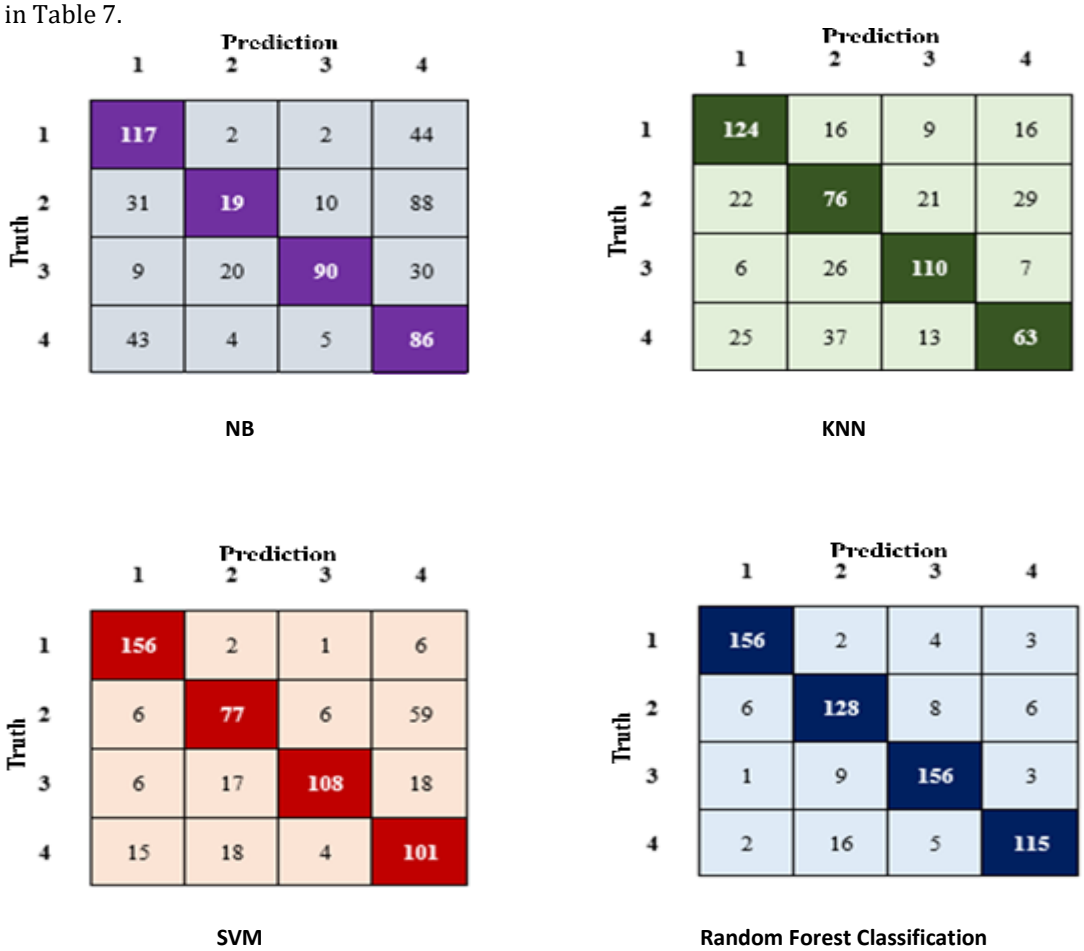


Figure 10. Confusion matrices of NB, KNN, SVM and RF algorithms for the case where all color spaces (RGB + HSV + YUV + LAB are used as the best combination

Figure 10 presents the confusion matrices of various classifiers implemented using all color space features (RGB + HSV + YUV + LAB). Each classifier shows different performance levels in terms of class prediction accuracy. (a) NB: This classifier shows relatively poor performance compared to others. There is a high level of misclassification, especially for classes 2 and 3. Class 2 instances are often mixed with classes 3 and 4, indicating that the probabilistic assumptions of NB do not match well with complex feature distribution. (b) KNN: KNN shows moderate performance with reasonable accuracy for classes 1 and 3. However, classes 2 and 4 suffer from confusion, especially with class 1. This may be due to the overlapping feature distributions in the multidimensional color space. (c) SVM: The SVM classifier shows strong performance with high accuracy across all classes. Especially for class 1 and class 3, the predictions are sharply concentrated on the diagonal, indicating the effective discrimination capabilities of the model in the feature space. (d) RF: RF achieved the best performance among all classifiers. The confusion matrix shows very high classification accuracy for all classes with minimal misclassification. This confirms the robustness and generalization ability of ensemble learning methods when using diverse and rich feature sets such as the combination of RGB, HSV, YUV and LAB color spaces.

Table 7. Comparison of the classification algorithms

| Classification algorithms | Accuracy (%) | Precision (%) | F1-Score (%) |
|---|---|---|---|
| NB | 52 | 55.37 | 50.20 |
| KNN | 62.17 | 61.81 | 61.86 |
| SVM | 73.67 | 75.27 | 73.60 |
| **RF** | **89.17** | **89.27** | **89.17** |

When Figure 10 and Table 7 are examined; the lowest accuracy value is seen in the NB classification algorithm with 52%. It is seen that the best accuracy value is with the proposed method, the RF algorithm, with 89.17%. These results prove that the RF algorithm is better than the NB, KNN and SVM classification algorithms.

## IV. CONCLUSION

The detection of underwater networks is very important to protect the underwater world. For this reason, various methods are being developed. In this study; Using the labels of the Network class from the SODD dataset and the Garbage, ROV, and Biological Living classes from the Trash Icra dataset, objects were cropped and a new dataset was created by randomly selecting 750 objects for each class from the cropped objects. Then, for each object in this dataset, the Energy, Similarity, Contrast, Homogeneity and Correlation textural features were extracted with the GLCM filter of the HSV, YUV, LAB, RGB color spaces. In the last step, these features were trained with the RF Algorithm. The results demonstrated that the RF algorithm outperformed NB, K-Nearest Neighbors (KNN), and Support Vector Machine (SVM) algorithms in capturing the complex and nonlinear patterns present in underwater imagery. Furthermore, various combinations of color spaces—from single to multiple—were tested, and it was observed that the use of combined color spaces significantly improved classification performance. This finding highlights the effectiveness of multi-color space approaches in processing underwater images. As a result of the training, it was seen that although each color space had a low accuracy value on its own, it positively affected the performance when used together and increased the accuracy, and the best accuracy value was 89.16% in the proposed method (HSV + YUV + LAB + RGB + GLCM). In addition, for the best case where all color spaces are used, NB, KNN and SVM classification algorithms were applied and the results were compared with the proposed method, RF. Accuracy values of 52% were obtained with NB, 62.17% with KNN and 73.67% with SVM, and it was proven that the best method was the proposed method, RF algorithm. However, the study has certain limitations. Although the dataset was constructed from two sources (SODD and Trash Icra), it may not comprehensively represent the variability of underwater environments. Moreover, the lighting conditions and other parameters across the two datasets may not be consistent. Additionally, the proposed method was not validated on any external or unseen datasets, which may limit the generalizability of the findings.

In future studies, the robustness and generalizability of the proposed method can be enhanced by applying optimization techniques for RF and other classifiers to potentially achieve higher accuracy and prevent overfitting, testing the method on different datasets and under varying environmental conditions, examining the effects of various parameter changes in the employed algorithms, and incorporating architectures such as CNNs to further improve performance.

## DECLARATIONS

**Acknowledgements:** The author/authors do not wish to acknowledge any individual or institution.

**Author Contributions:** Conceptualization, N.N.A, G.K. and O.Y.; Methodology, N.N.A. and O.Y..; Validation, C.D.; Investigation, N.N.A, G.K. and O.Y; Resources, N.N.A, G.K.; Data Curation, N.N.A, G.K. and O.Y.; Writing—Original Draft, N.N.A, G.K. and O.Y.; Writing—Review & Editing, N.N.A, G.K. and O.Y.; Supervision, O.Y. All authors have read and approved the final version of the manuscript.

**Conflict of Interest Disclosure:** The author/authors declare no conflict of interest.



**Funding/Supporting Organizations:** This research received no external funding.

**Ethical Approval and Participant Consent:** This study does not involve human or animal participants. All procedures followed scientific and ethical principles, and all referenced studies are appropriately cited.

**Plagiarism Statement:** This article has been evaluated for plagiarism and no instances of plagiarism were detected.

**Availability of Data and Materials**: Data sharing is not applicable to this study.

**Use of AI Tools:** The authors declare that no Artificial Intelligence (AI) tools were used in the creation of this article.

## V. REFERENCES

Akbulut, H., Atasever, S., & Sıramkaya, E. (2025). Makine öğrenmesine dayalı portakal kalite sınıflandırması: Puma optimize edici ile bir hiperparametre optimizasyon yaklaşımı. In *7th International Conference on Human-Computer Interaction, Optimization and Robotic Applications (ICHORA).* (pp. 1–5). https://doi.org/10.1109/ICHORA65333.2025.11017028

Al-Tairi, Z. H., Rahmat, R. W., Saripan, M. I., & Sulaiman, P. S. (2014). Skin segmentation using YUV and RGB color spaces. *Journal of Information Processing Systems. 10*(2), 283–299. https://doi.org/10.3745/JIPS.02.0002

Apaydın, N. N., Apaydın, M.,& Yaman, O. (2022). Su altı görüntülerinden adli delil tespiti için LBP tabanlı sınıflandırma yöntemi. *Fırat Üniversitesi Uzay ve Savunma Teknolojileri Dergisi. 1*(1), 272-276.

Belgiu, M., & Drăguţ, L. (2016). Random forest in remote sensing: A review of applications and future directions. *ISPRS Journal of Photogrammetry and Remote Sensing. 114*, 24–31. https://doi.org/10.1016/j.isprsjprs.2016.01.011

Character, L., Ortiz, A., Jr., Beach, T., & Luzzadder-Beach, S. (2021). Archaeologic machine learning for shipwreck detection using LiDAR and sonar. *Remote Sensing. 13*(9), Article 1759. https://doi.org/10.3390/rs13091759

De Langis, K., Fulton, M., & Sattar, J. (2020). An analysis of deep object detectors for diver detection. *arXiv.* https://doi.org/10.48550/arXiv.2012.05701

Demir, K., & Yaman, O. (2024a). A HOG feature extractor and KNN-based method for underwater image classification. *Fırat University Journal of Experimental and Computational Engineering (FUJECE). 3*(1), 1–10. https://doi.org/10.62520/fujece.1443818

Demir, K., & Yaman, O. (2024b). Projector deep feature extraction-based garbage image classification model using underwater images. *Multimedia Tools and Applications. 83*(33), 79437–79451. https://doi.org/10.1007/s11042-024-18731-w

Fulton, M. S., Hong, J., & Sattar, J. (2020). Trash-ICRA19: A bounding box labeled dataset of underwater trash [Data set]. *Data Repository for the University of Minnesota (DRUM).* https://doi.org/10.13020/x0qn-y082

Han, F., Yao, J., Zhu, H., & Wang, C. (2020). Underwater image processing and object detection based on deep CNN method. *Journal of Sensors.* 2020, 1–20. https://doi.org/10.1155/2020/6707328

Imam, H. M. A., Basso, E. A., Hoff, S. A., Rexha, H., Lafond, S., & Iancu, B. (2023, November 30). SODD – subaquatic object detection dataset [Data set]. *Zenodo.* https://doi.org/10.5281/zenodo.10230328

Kim, J., Kim, T., Kim, J., Rho, S., Song, Y., & Yu, S.-C. (2019a). Simulation and feasibility test of mini-ROVs with AUV for the manipulation purpose. *OCEANS 2019 MTS/IEEE SEATTLE.* (pp. 1–6). https://doi.org/10.23919/OCEANS40490.2019.8962810

Kim, J., Kim, T., Kim, J., Yu, S.-C., & Kim, T. (2019b). Manipulation purpose underwater agent vehicle for ghost net recovery mission. *2019 IEEE/RSJ International Conference on Intelligent Robots and Systems (IROS).* (pp. 3905–3910). https://doi.org/10.1109/IROS40897.2019.8967625

Mohanaiah, P., Sathyanarayana, P., & GuruKumar, L. (2013). Image texture feature extraction using GLCM approach. *International Journal of Scientific and Research Publications.* Volume 3, Issue 5, May 2013 1, ISSN 2250-3153

Morishige, C., & McElwee, K. (2012). At-sea detection of derelict fishing gear in the North Pacific: An overview. *Marine Pollution Bulletin. 65*(1–3), 1–6. https://doi.org/10.1016/j.marpolbul.2011.05.011

Raveendran, S., Patil, M. D., & Birajdar, G. K. (2021). Underwater image enhancement: A comprehensive review, recent trends, challenges and applications. *Artificial Intelligence Review. 54*(7), 5413–5467. https://doi.org/10.1007/s10462-021-10025-z

Rijkure, A., & Megnis, J. (2024). Technical methods of cleaning shipwrecks from ghost nets. *Environmental and Technology Resources: Proceedings of the International Scientific and Practical Conference.(* Vol. 3, pp. 253–256). https://doi.org/10.17770/etr2024vol3.8160

Shaik, K. B., Ganesan, P., Kalist, V., Sathish, B. S., & Jenitha, J. M. M. (2015). Comparative study of skin color detection and segmentation in HSV and YCbCr color space. *Procedia Computer Science. 57*, 41–48. https://doi.org/10.1016/j.procs.2015.07.362

Spirkovski, Z., Ilik-Boeva, D., Ritterbusch, D., Peveling, R., & Pietrock, M. (2019). Ghost net removal in ancient Lake Ohrid: A pilot study. *Fisheries Research. 211*, 46–50. https://doi.org/10.1016/j.fishres.2018.10.023

Valdenegro-Toro, M. (2016, December). Submerged marine debris detection with autonomous underwater vehicles. *In 2016 International Conference on Robotics and Automation for Humanitarian Applications (RAHA).* (pp. 1–7). https://doi.org/10.1109/RAHA.2016.7931907

Wei, C., Bai, Y., Liu, C., Zhu, Y., Wang, C., & Li, X. (2024). Unsupervised underwater shipwreck detection in side-scan sonar images based on domain-adaptive techniques. *Scientific Reports. 14*(1), Article 12687. https://doi.org/10.1038/s41598-024-63501-1

Yaman, O., Yetis, H., & Karakose, M. (2020). Band reducing based SVM classification method in hyperspectral image processing. *2020 Zooming Innovation in Consumer Technologies Conference (ZINC).* (pp. 21–25). https://doi.org/10.1109/ZINC50678.2020.9161813

Yang, F.-J. (2018). An implementation of Naive Bayes classifier. *2018 International Conference on Computational Science and Computational Intelligence (CSCI).* (pp. 301–306). https://doi.org/10.1109/CSCI46756.2018.00065

Ye, X., & Wang, X. (2018, July). Deep generative network and regression network for fishing nets detection in real-time. *2018 37th Chinese Control Conference (CCC).* (pp. 9466–9471). https://doi.org/10.23919/ChiCC.2018.8483142

Yuan (Zhang), Y., Dong, Z., Zhang, K., Shu, S., Lu, F., & Chen, J. (2021, January). Illumination variation-resistant video-based heart rate monitoring using LAB color space. *Optics and Lasers in Engineering. 136*, Article 106328. https://doi.org/10.1016/j.optlaseng.2020.106328

Yuh, J., & West, M. (2001, January). Underwater robotics. *Advanced Robotics. 15*(5), 609–639. https://doi.org/10.1163/156855301317033595

Zhang, Y., Wang, X., Sun, L., Lei, P., Chen, J., He, J., Zhou, Y., & Liu, Y. (2024). Mask-guided deep learning fishing net detection and recognition based on underwater range gated laser imaging. *Optics and Laser Technology. 171*, Article 110402. https://doi.org/10.1016/j.optlastec.2023.110402

Zhao, Y.-P., Niu, L.-J., Du, H., & Bi, C.-W. (2020). An adaptive method of damage detection for fishing nets based on image processing technology. *Aquacultural Engineering. 90*, Article 102071. https://doi.org/10.1016/j.aquaeng.2020.102071

Zuzanna, K., Tomasz, U., Michał, G., & Robert, P. (2022). How high-tech solutions support the fight against IUU and ghost fishing: a review of innovative approaches, methods, and trends. *IEEE Access, 10*, 112539-112554. https://doi.org/10.1109/ACCESS.2022.3212384